Benchmarking of novel green fluorescent proteins for the quantification of protein oligomerization in living cells

Annett Petrich[1], Amit Koikkarah Aji[1], Valentin Dunsing[1,2], Salvatore Chiantia[1,‡]

[1] University of Potsdam, Institute of Biochemistry and Biology, Karl-Liebknecht-Straße 24-25, 14476 Potsdam, Germany

[2] Aix-Marseille University, CNRS, UMR 7288, IBDM, Turing Center for Living Systems, Marseille, France

[‡] Correspondence: chiantia@uni-potsdam.de

Abstract

Protein-protein-interactions (PPIs) play an important role in several cellular functions. Quantitative non-invasive techniques are applied in living cells to evaluate PPIs, thereby providing a broader understanding of complex biological processes. Fluorescence fluctuation spectroscopy (FFS) describes a group of quantitative microscopy approaches for the characterization of PPIs at single cell resolution. Through the obtained molecular brightness, it is possible to determine the oligomeric state of proteins. This is usually achieved by fusing fluorescent proteins (FPs) to the protein of interest. Recently, the number of novel green FPs has increased, with consequent improvements to the quality of FFS measurements. The photophysical behavior of FPs is influenced by multiple factors (including photobleaching, protonation-induced "blinking" and long-lived dark states). Assessing these factors is critical for selecting the appropriate fluorescent tag for live cell imaging applications. In this work, we focus on novel green FPs that are extensively used in live cell imaging. A systematic performance comparison of several green FPs in living cells under different pH conditions using number & brightness (N&B) analysis and scanning fluorescence correlation spectroscopy (sFCS) was performed. Our results show that the new FP Gamillus exhibits higher brightness at the cost of lower photostability and fluorescence probability (*pf*), especially at lower pH. mGreenLantern, on the other hand, thanks to a very high *pf*, is best suited for multimerization quantification at neutral pH. At lower pH, mEGFP remains apparently the best choice for multimerization investigation. These guidelines provide the information needed to plan quantitative fluorescence microscopy involving these FPs, both for general imaging or for PPI quantification via FFS.

Keywords

Fluorescence correlation spectroscopy, fluorescence microscopy, fluorescence fluctuation spectroscopy, number and brightness, fluorescent proteins, multimerization, quantitative microscopy

Abbreviations

FFS, fluorescence fluctuation spectroscopy; FP, fluorescence protein; N&B, number and brightness; *pf*, fluorescence probability; PM, plasma membrane; PPI, protein-protein-interaction; sFCS, scanning fluorescence correlation spectroscopy

Introduction

A multitude of cellular processes, such as biomolecule transport, ion channel activity, cell-cell adhesion and communication are regulated by protein-protein-interactions (PPIs) [1-3]. "Classical" bulk biochemical *in vitro* methods that are used to quantify PPIs (e.g., co-immunoprecipitation (co-IP), pull-down assays and western blotting) cannot be used to obtain information about intracellular protein distribution in live-cell samples or to monitor the effects of variations in concentrations between different cells [4, 5]. Conventional optical microscopy can visualize the localization of proteins, but its resolution is limited [4, 6]. More complex approaches, such as fluorescence fluctuation spectroscopy (FFS), can assess the interactions between molecules in complexes and obtain insights into cellular pathways and assembly processes [4-8]. FFS provides information about dynamics through the analysis of signal fluctuations from fluorescently labeled molecules [6, 7, 9]. Additionally, the magnitude of such fluctuations can be used to derive quantitative information about the multimerization state (i.e., number of monomers in a multimer) of the protein of interest [7-10].

A common strategy to investigate PPIs *in cellula* via FFS is the fusion of a fluorescent protein (FP) to the protein of interest [7-9, 11]. Comparison between the brightness of protein multimers tagged with FPs and the brightness of a monomeric reference allows the quantification of FP monomers in the complex and, thus, the oligomerization state of the protein of interest [5, 7, 12]. A major problem for several FFS applications that rely on FPs, though, is the presence of non-emitting "dark" proteins, which can be quantified through the so-called fluorescence probability (*pf*) [7, 13]. It is sometime assumed that FPs have a *pf* value of 1 meaning that, for example, a trimer containing three FPs emits in average a three-fold higher signal than a monomer labelled with one FP [5, 7]. Instead, *pf* values of e.g. green emitting FPs have been reported in the range between 0.5 and 0.8 [1, 2, 7, 13-19]. Recently, we have systematically quantified the *pf* of several FPs, focusing mainly on proteins emitting in the red part of the visible spectrum [7]. In summary, since high *pf* values are required for increased sensitivity, not all FPs are equally suitable for oligomerization studies [7]. Because of the presence of non-emitting FPs (i.e., *pf* lower than 1), FFS approaches might underestimate the amount of FPs and therefore, the oligomeric state of the protein of interest.

Some of the most used FPs are the green fluorescent protein (GFP) and its mutants, such as the monomeric enhanced GFP (mEGFP) [5, 20]. This FP has a high quantum yield (QY), enhanced photostability, and minimal interference with the cellular machinery [20]. Of note, several variants have been engineered over the past few years (e.g. mNeonGreen (mNG), mGreenLantern (mGL), and Gamillus) in an effort to optimize molecular brightness, folding efficiency, photostability, and pH stability of the fluorescent probe (Table 1) [21-24].

70 **Table 1 Photophysical characteristics of the fluorescence proteins (FPs).** QY, Quantum yield.

FP	λ_{ex} [nm]	λ_{em} [nm]	QY	Brightness*	cellular norm. <I>	pK_a	maturation [min]	Reference
mEGFP	488	507	0.71	38.0	1.0[#,†]	6.0	28.0	[21]
mNG	506	516	0.78	90.0	3.3[#]	5.7	18.0	[21]
mGL	503	514	0.72	74.0	6.3[#]	5.6	14.0	[21]
Gamillus	504	519	0.90	74.7	0.5[†]	3.4	8.0	[24]

71 [*] (extinction coefficient × QY)/1,000, where QY and extinction coefficients are measured at the absorbance peak (λ_{ex} ± 2 nm)
72 [#] Average intensity in FP-expressing BE (2)-M17 human neuroblastoma cells, relative to EGFP, using the P2A quantitative co-expression system
73 [†] Average intensity in FP-expressing HeLa cells, relative to EGFP

74

75 In the context of complex experiments in living cells, a FP might encounter different environments and pH
76 conditions (e.g. acidic pH in lysosomes, secretory granule and endosomes; neutral pH in the nucleus,
77 cytoplasm and endoplasmic reticulum (ER); basic pH in mitochondria and a pH gradient in the Golgi
78 network) [22, 25]. Measurements of GFP at acidic pH have shown a decrease of the *pf* value, possibly due
79 to an increase of proteins in the dark-state [22, 26-28]. Consequently, it would be useful to systematically
80 analyze the properties of the above-mentioned novel FPs, in order to perform an exact quantification of
81 PPIs, also in different intra-cellular environments.

82 Here, we benchmarked the performance of novel green FPs (mGL and Gamillus) against the well-
83 established mEGFP and mNG. The presence of non-fluorescent states and photostability under different
84 pH conditions was measured using Number & Brightness (N&B) and scanning fluorescence correlation
85 spectroscopy (sFCS) analysis [5]. Our results indicate that some of the observed proteins are brighter,
86 although unstable under longer/stronger illumination. Furthermore, we identify which proteins are more
87 suitable for multimerization quantification, rather than "simple" imaging, also at different pH conditions.

88

Materials and Methods

Fluorescent protein constructs

A detailed description of the cloning procedure of all constructs is available in the supplementary material. All plasmids generated for this work will be made available on Addgene (https://www.addgene.org/). A schematic overview of the intracellular localization of the constructs is provided Figure S1A and an overview of the linker sequences within the FP structures is provided in Table S1.

Cell culture

Human embryonic kidney cells from the 293T line (HEK293T, CRL-3216™) and Chinese hamster ovary cells (CHO-K1, CCL-61™) were purchased from ATCC (Kielpin Lomianki, Poland). Both cell lines were cultured in phenol red-free Dulbecco's modified Eagle's medium (DMEM) with 10% fetal bovine serum, 2 mM L-glutamine, 100 U/mL penicillin, and 100 mg/mL streptomycin at 37 °C and 5% CO_2. Cells were passaged every 2–3 days when they reached nearly 80% confluence in tissue culture flask, for 15 passages. All solutions, buffers, and media used for cell culture were purchased from PAN-Biotech (Aidenbach, Germany).

Preparation for Microscopy Experiments

For microscopy experiments, 6×10^5 (HEK293T) or 4×10^5 (CHO-K1) cells were seeded in 35 mm dishes (CellVis, Mountain View, CA, USA) with optical glass bottom (#1.5 glass, 0.16–0.19 mm), 24 h before transfection. HEK293T cells are preferred for sFCS measurements since they are relatively thick and therefore suitable for sFCS based data acquisition perpendicular to the PM. CHO-K1 cells are rather flat and characterized by a large cytoplasmic volume and therefore suitable for N&B measurements in the cytoplasm. Cells were transfected 16–24 h prior to the experiment using 200 ng plasmid DNA per dish with Turbofect (Thermo Fisher Scientific, Waltham, MA, USA) according to the manufacturer's instructions.

For measurements under different pH conditions, the culture medium was exchanged with buffer containing 140 mM NaCl, 2.5 mM KCl, 1.8 mM $CaCl_2$, 1.0 mM $MgCl_2$, and 20 mM HEPES with a pH value of 5.6, 7.4 or 9.2.

Confocal microscopy system and setup calibration for fluorescence fluctuation spectroscopy

All measurements were performed on a Zeiss LSM780 system (Carl Zeiss Microscopy GmbH, Oberkochen, Germany) using a Plan-Apochromat 40×/1.2 Korr DIC M27 water immersion objective and a 32-channel GaAsP detector array. Samples were excited with a 488 nm Argon laser and the fluorescence signal was collected in a range of 498 to 606 nm in photon-counting mode after passing through a 488 nm dichroic mirror. For the spectral analysis under different pH conditions, fluorescence was detected in spectral channels of 8.9 nm width (23 channels between 491 nm and 690 nm). To decrease out-of-focus light, a

pinhole with size corresponding to one airy unit was used. All measurements were performed at 22 ± 1 °C.

The confocal volume was calibrated daily by performing a series of point FCS measurements with Alexa Fluor® 488 (AF488, Thermo Fischer, Waltham, MA, USA) dissolved in water at 30 nM, at the same laser power and beam path used for N&B and sFCS measurements. Prior to that, the signal was optimized by adjusting the collar ring of the objective and the pinhole position to the maximal count rate for AF488. Then, five measurements at different locations were acquired, each consisting of 15 repetitions of 10 s, and the data was fitted using a three-dimensional diffusion model including a triplet contribution. The structure parameter S (defined as the ratio between the vertical and lateral dimension of the theoretical confocal ellipsoid) was typically around 5 to 9, and the diffusion time τ_d around 30 to 35 µs.

N&B measurements

N&B analysis was performed as previously described [7, 10] with few modifications: 128x 128 pixel images were acquired with pixel dimensions of 400 nm and a pixel dwell time of 50 µs. Image time-stacks of 105 scans were collected using the Zeiss Black ZEN software. The intensity time-stacks data were analyzed using a custom Matlab code (The MathWorks, Natick, MA, USA). The Matlab algorithm utilizes the equations from Digman *et al.* [11] for obtaining the molecular brightness and number as a function of pixel position. Bleaching and minor cell movements are partially corrected using a boxcar-filter with an 8-frame window applied pixel-wise, as previously described [7, 29, 30]. Final brightness values were calculated by extrapolating the partial brightness values (i.e., calculated within each 8-frame window) to the earliest time point. Detector saturation leading to artefactual reduction in brightness was avoided by excluding pixels with photon-counting rates exceeding 1 MHz. A schematic overview of the N&B analysis is provided in Figure S1C.

sFCS measurements

Scanning FCS experiments were performed as previously described [7, 31], with a modified acquisition mode. Briefly, a line scan of 256 × 1 pixels (pixel size ~80 nm) were performed perpendicular to the membrane with 472.73 µs scan time. Typically, 400,000 lines were acquired (total scan time ~3 min) in photon counting mode. Laser power values were typically between ~1.5 µW (brightness analysis) and ~6 µW (photobleaching analysis). Scanning data were exported as TIFF files, imported and analyzed in MATLAB (The MathWorks, Natick, MA, USA) using a custom code as previously described [7, 31, 32]. A schematic overview of the sFCS analysis is provided in Figure S1D.

Brightness calibration and fluorophore maturation

The molecular brightness, i.e. the photon count rate per molecule, is used as a measure for the oligomeric state of protein complexes. This quantity is often based on the assumption that all fluorophores within an oligomer are fluorescent. However, FPs can undergo dark state transitions or be in a non-mature, non-

fluorescent state [8]. To quantify the amount of non-fluorescent FPs, we consider all these processes together in a single parameter, the apparent fluorescence probability (*pf*), i.e. the probability of a FP to emit a fluorescence signal. The determination of the *pf* value from apparent brightness values was performed as previously described [7, 32]. Shortly, for each sample and each experiment day, the average brightness for a monomeric construct was determined from a large number of cells. Then, several measurements were performed in cells expressing the dimer constructs and, from each of these measurements and the monomer brightness obtained before, one *pf* value was calculated as discussed before [7, 32]. The final *pf* value was calculated as mean of such a set of measurements (see Figures 2B and 3B).

Statistical analysis

Data from at least three independent experiments were pooled and visualized using GraphPad Prism ver. 9.0.0 (GraphPad Software, LCC, San Diego, CA, USA). All resulting data were displayed as box plots with single data points corresponding to measurements in single cells or as mean ± standard error of the mean (SEM) plots. Median values and whiskers ranging from minimum to maximum values are displayed in the box plots. The mean, median, interquartile range (IQR) are indicated in each graph together with the sample size. Significance values are given in each graph and figure captions, respectively. Statistical significance was tested by using D'Agostino-Pearson normality test followed by one-way ANOVA analysis and the Tukey's or Fishers Least Significant Difference (LSD) multiple comparisons test.

Code availability

MATLAB custom-written code is available from the corresponding author upon reasonable request.

Data availability

The datasets analyzed during the current study are available from the corresponding author upon reasonable request.

Results

mGL and Gamillus are less photostable than mEGFP or mNG

All FPs were evaluated for photostability at different laser powers using confocal microscopy, in the context of a typical N&B experiment performed in CHO-K1 cells. Such an approach simply consists of a time-series acquisition with continuous scanning over ca. two minutes. mGL and Gamillus displayed higher photobleaching, both in the cytosol and at the PM, in comparison to mEGFP and mNG (Figure 1A and 1B, Table S2). For example, ≈30% of the total mGL was bleached after a ca. two-minute of continuous scanning, using 2.4 µW excitation power. At the same time, N&B analysis provided the brightness of each FP, as a function of the laser power. Although an accurate analysis should be performed at an excitation power causing as low as possible bleaching (see next paragraph), Figures 1C and D confirm that the observed brightness predictably increases roughly linearly with the laser power. As expected, due to the detection geometry, a higher signal is observed for molecules restricted to the PM [33]. Finally, Gamillus shows generally a higher brightness, as especially noticeable for measurements at the PM or at higher excitation powers.

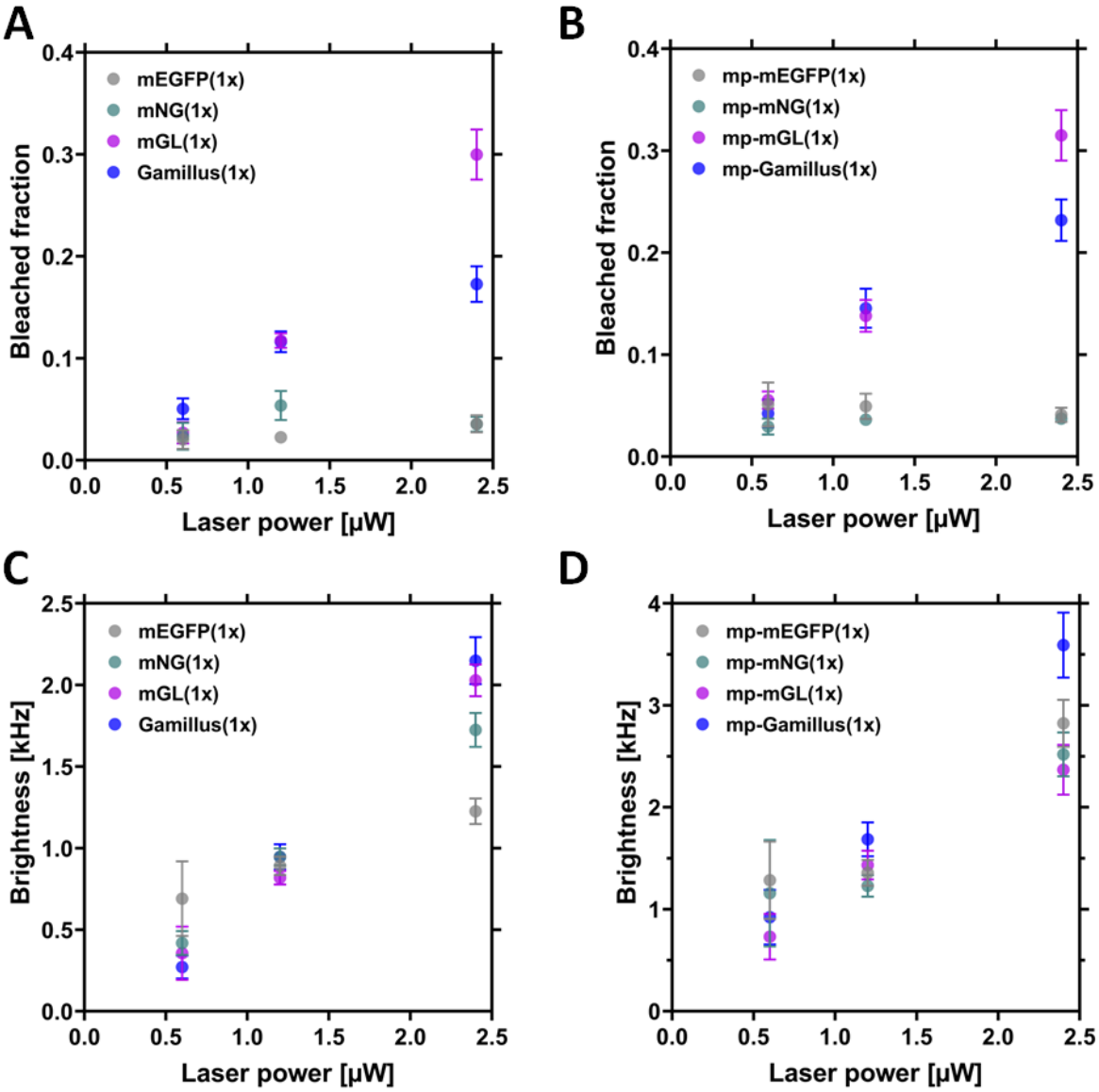

196

197 **Figure 1: Comparison of the molecular brightness and bleached fraction for the examined FPs, as obtained from N&B**
198 **measurements in CHO-K1 cells.** CHO-K1 cells were transfected with plasmids coding for the monomeric cytosolic FPs (mEGFP(1x),
199 mNeonGreen(1x) (here, called mNG(1x)), mGreenLantern(1x) (here called mGL(1x)) and Gamillus(1x)) or with membrane-
200 anchored FPs. The latter are anchored to the inner leaflet of the PM via a myristoylated and palmitoylated (mp) peptide (mp-
201 mEGFP(1x), mp-mNG(1x), mp-mGL(1x) or mp-Gamillus(1x)). N&B measurements were performed ≈16 h after transfection with a
202 laser power of 0.6 µW, 1.2 µW and 2.4 µW. (A-B): Mean bleached fractions measured for cytosolic FPs (A) and for PM-anchored
203 FPs (B), as a function of laser power. The bleached fraction indicates the amount of fluorescence signal lost after a N&B
204 measurement. Error bars indicate the standard error of the mean (SEM). (C-D): Mean brightness values measured for cytosolic
205 FPs (C) and for PM-anchored FPs (D), as a function of laser power. Error bars represent the SEM. Exact values and sample sizes
206 are summarized in Table S2.

207

Gamillus exhibits high brightness but low fluorescence probability

To compare the brightness effectively observed in a typical confocal microscopy setup and, specifically, in the context of FFS experiments, we have performed in-depth N&B analysis of FP monomer and dimer constructs. In order to maintain bleaching below ≈15%, we have excited the fluorophores with a laser power of 1.2 µW. CHO-K1 cells were transfected with the required plasmids and observed after 16 h. Figure 2A shows the brightness values measured for the different FP monomer constructs, either in the cytosol or at the PM. The results follow, as expected, the general trend already described above (Figures 1C and D). No significant difference can be observed between brightness values at this low laser power, with the exception of mp-Gamillus displaying a higher brightness than the other membrane-associated constructs.

Next, we have performed similar experiments on dimer constructs of the same FPs (Figure S2A), in order to calculate the *pf*, as shown in Figure 2B. All *pf* values are in the expected range, around 0.7, and no large difference can be observed between the different fluorophores in general. Noticeably though, mp-Gamillus exhibits *pf* values lower than those of the other FPs (in particular, significantly lower than mp-mGL, ca. 0.6 vs. ca. 0.9).

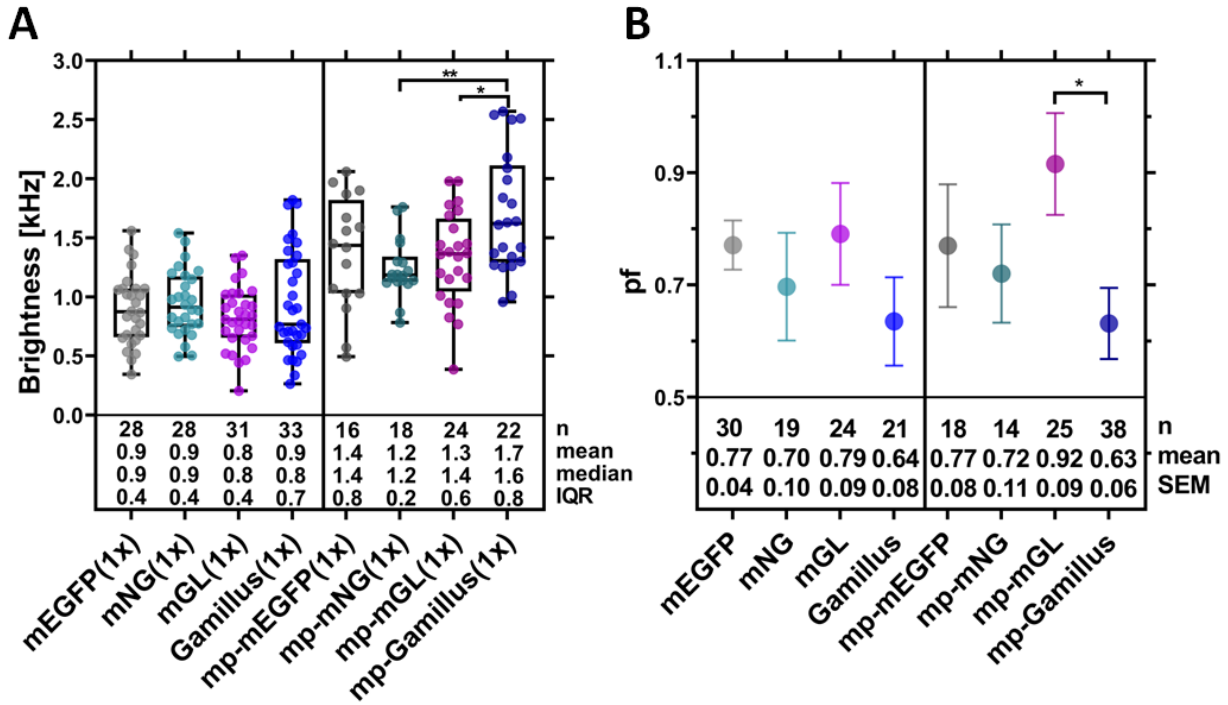

Figure 2: Comparison of brightness and fluorescence probability (*pf*) for the examined green FPs, as obtained from N&B measurements in CHO-K1 cells. N&B measurements were performed ≈16 h after transfection, using a laser power of 1.2 µW. (A): Box plot of the molecular brightness for the examined cytosolic and membrane-anchored FPs (i.e., mp-FP). Each point represents the average value measured in a single cells, from three independent experiments. Median values and whiskers ranging from minimum to maximum values are displayed. (B): Mean *pf* values calculated for the cytosolic and membrane-anchored FPs, using the brightness values measured for the corresponding FP dimers (Figure S2A). Data were collected from three independent experiments. The error bars represent the SEM. Sample size, mean/median, and interquartile range (IQR)/SEM

are indicated below the graph. Statistical significance within both plots for selected sample pairs were determined using one-way ANOVA Tukey´s multiple comparison test (* $p < 0.05$, ** $p < 0.005$). Values obtained from independent experiments are indicated in Table S3.

Performance comparison of FPs at different pH values

The fluorescence emission intensity of some FPs often decreases at low pH values due to protonation of the chromophore [22, 24, 26]. Protonation can induce the transition to dark states and, therefore, negatively affect the accuracy of molecular brightness measurements [28]. Here, the pH-dependent fluorescence of the FPs was analyzed via confocal microscopy in the pH range from 5.6 to 9.2 in HEK293T cells using constructs associated to the outer side of the PM via a glycosylphosphatidylinositol (GPI) anchor. The fluorescence emission spectra of the different FPs did not change considerably in the assessed pH range and no photoconversion was observed (Figure S3). Also, the photostability of the FP variants at different pH conditions was qualitatively compared (Figure S4) using an excitation power of 6 µW, on a specific position of the PM, for ca. 3 minutes. This configuration is usually employed for FCS measurements at the PM and is different from the N&B whole-frame scanning approach used for the experiments described in the previous paragraphs [10]. GPI-mEGFP showed a good photostability at all pH conditions, with the fluorescence signal decreasing by only ca. 20% (Figure S4A). GPI-mNG(1x) exhibited fast initial photobleaching, particularly at pH values 5.6 and 9.2, down to ca. 50% of the original signal. At neutral pH, bleaching of GPI-mNG was only slightly higher than that of GPI-mEGFP (Figure S4B). A fast and substantial photobleaching, especially at neutral and low pH was observed for GPI-mGL (Figure S4C). Finally, as shown in Figure S4D, a strong pH-dependency of photostability was observed for GPI-Gamillus: at the highest pH the bleaching was minor (i.e., ca. 20%, similar to GPI-mEGFP), while at neutral and low pH the emission signal dramatically decreased (i.e., to ca. 40% and 10% at pH 7.4 and 5.6, respectively). Overall, mEGFP showed the highest photostability for all pH conditions followed by mNG and then mGL and Gamillus (pH < 9.2), in agreement with the results from N&B analysis (Figure 1B).

Additionally, the molecular brightness of the different FPs under various pH conditions was evaluated for monomer and dimer membrane-associated GPI-anchored constructs, and the corresponding *pf* values were determined (Figure 3 and S2B, Table S4). To complement the previous experiments, we used an alternative FFS approach (i.e., sFCS [34]) and an alternative live-cell model (i.e., HEK293T) for this set of experiments. sFCS experiments result in fluorescence auto-correlation curves which can be analyzed to extract parameters such as diffusion coefficients of the labelled proteins, concentration and molecular brightness (see Figure S5 for representative examples). As shown in Figure 3A, the results obtained at pH 7.4 corroborate what was observed also via N&B (Figures 1D and 2A), i.e. that Gamillus overall exhibits a higher brightness compared to the other FPs. This observation holds true for all the tested pH conditions. In general, the observed brightness values did not differ much among each other (being all within a ca. 15% variation interval) and we did not observe an effect of pH, at least at the low laser powers used here.

More marked differences were observed, however, for the *pf* values. In general, this parameter showed a negative correlation with increasing pH for GPI-mEGFP and a positive correlation for GPI-Gamillus. No strong correlation was observed instead for GPI-mGL or GPI-mNG. At pH 5.6, the *pf* of GPI-Gamillus was

270 significantly lower than that of GPI-mEGP and, overall, the lowest among all investigated proteins. At
271 neutral pH, GPI-mGL showed the best performance, in agreement with what we observed for mp-mGL via
272 N&B (Figure 2B). At pH 9.2, no strong differences were observed in general among all FPs, although GPI-
273 Gamillus displayed by trend the highest *pf* value. Notably, we did not observe pH-induced changes in the
274 autocorrelation functions (indicating e.g. significant alterations in the triplet state fraction) for any FP, at
275 this low excitation power (Figure S5). An in-depth study of fluorescence intensity dynamics faster than ca.
276 1 ms would require, in general, approaches with higher temporal resolution.

277

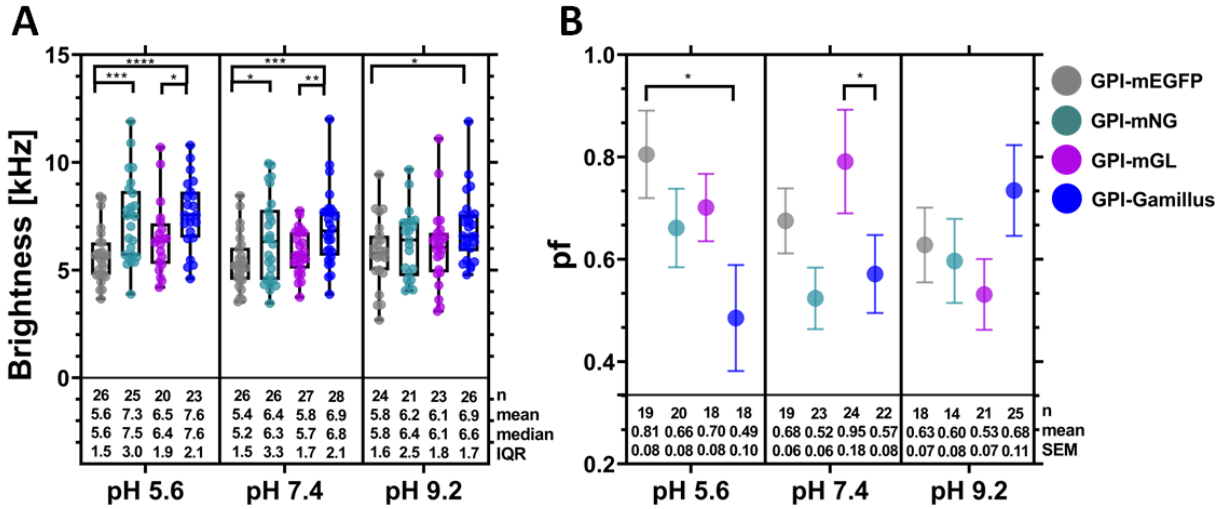

278

279 **Figure 3: Comparison of brightness and *pf* values for the examined FPs, as obtained from scanning fluorescence correlation**
280 **spectroscopy (sFCS) measurements in HEK293T cells, under different pH conditions (pH 5.6, pH 7.4, and pH 9.2).** sFCS
281 measurements were performed ≈16 h after transfection, using a laser power of 1.5 µW. (A): Box plots of the molecular brightness
282 for the membrane-anchored FPs GPI-mEGFP , GPI-mNG , GPI-mGL and GPI-Gamillus, for three different pH conditions. Each point
283 represents the average value measured in single cells, from three independent experiments. Median values and whiskers ranging
284 from minimum to maximum values are displayed. (B): Average *pf* values calculated using the brightness values measured for the
285 corresponding FP dimers (Figure S4), for three different pH conditions. Data were collected from three independent experiments.
286 The error bars represent the SEM. Statistical significance was determined for selected sample pairs in both plots using one-way
287 ANOVA Fishers Least Significant Difference (LSD) multiple comparison test (* $p < 0.05$, ** $p < 0.005$, *** $p < 0.0005$, **** $p <$
288 0.0001). Values obtained from independent experiments are indicated in Table S4.

289

290 # Discussion

291 PPIs and, specifically, homo-multimerization can be quantified directly in living cells using quantitative
292 fluorescence microscopy approaches based on FFS (e.g., sFCS and N&B) [6-8]. The molecular brightness
293 (i.e., photon count rate per molecule) derived from such experiments allows the determination of the
294 oligomeric state of FP-tagged protein complexes. [7, 8, 10]. The reliability of such approaches is influenced
295 by the photophysical behavior of the FPs, which can be summed up by the *pf* parameter [7]. The *pf* is
296 determined by the specific experimental conditions (e.g. excitation wavelength and power, duration of
297 illumination, geometry of the detection volume), sample environment (pH, ion composition, etc.),
298 intracellular biochemical processes (e.g. maturation time and folding efficiency) and photophysical
299 processes (photobleaching, quantum yield, triplet state formation, protonation- or light-induced
300 "blinking", long-lived dark states, etc.) [9, 20, 26-28, 34-40]. Therefore, three requisites should be ideally
301 met by FPs used in typical FFS studies: i) high photostability, essential to allow time-based measurements
302 under continuous illumination, ii) high molecular brightness, required to achieve sufficient signal-to-noise
303 ratio to detect single molecule fluctuations and iii) a high *pf*, crucial for a large dynamic range and accuracy
304 of oligomerization measurements. In this study, we present a comprehensive analysis of novel GFP
305 variants (mGL and Gamillus) and their suitability for brightness-based oligomerization studies. Both
306 proteins were reported to mature remarkably quickly and to possess a high brightness and medium-low
307 acid sensitivity compared to mEGFP (see Table 1) [21, 24], thus suggesting that they are promising
308 candidates for quantitative FFS studies. These features are, at least partially, shared also by the
309 established GFP variant mNG [23], which is therefore also included in this study.

310 Previous studies have characterized these FPs and compared them to e.g. mEGFP as standard (see e.g.
311 [41]). Nevertheless, it must be noted that essential parameters, such as brightness, pH sensitivity or
312 photostability, are often measured with different methods and the outcome might depend on the specific
313 setup [23, 24, 41-43]. Thus, it is reasonable to compare the FPs systematically using specific conditions
314 and approaches resembling those of actual FFS experiments. Following this logic, we used typical FFS
315 approaches (i.e., N&B and sFCS) to quantify the stability, brightness, pH sensitivity and *pf* of mEGFP, mNG,
316 Gamillus and mNG.

317 A first unexpected result is that, in general, we do not observe strikingly different brightness values
318 between each FP. While this observation can likely be explained by the distinctive experimental setup
319 (e.g. very low excitation power, longer acquisition times, specific intra-cellular localization [21, 42, 44]), it
320 is nevertheless relevant for users planning similar FFS-based investigations. Furthermore, the brightness
321 measured via FFS is an average value derived from a statistical analysis of single molecule fluctuations.
322 Such analysis is different from bulk methods that measure the fluorescence emission in a whole cell as a
323 readout of brightness. While remaining both valid, the different approaches might provide information
324 about different aspects of the fluorescent system. Finally, in our experimental conditions, Gamillus
325 displayed a higher brightness compared to the other FPs, at least when located at the PM or while using
326 higher laser powers. This observation was independently confirmed via both sFCS and N&B analysis.

327 Both techniques also indicate that the higher brightness of Gamillus is counterbalanced by a stronger
328 tendency to photobleach, at least in the conditions used in our experiments (e.g., pH 7.4). A similarly low

329 photostability was observed also for mGL, while mNG and mEGFP proved to be remarkably stable under
330 continuous irradiation. Of interest, the contrast with reports indicating a strong photostability of mGL and
331 Gamillus might be only apparent. A general comparison of these observations with previous studies is
332 complicated by the fact that, often, different conditions and experimental setups result in different
333 apparent photochemical behavior. For example, mEGFP was shown to be less stable than mNG under
334 widefield illumination, more stable under laser illumination [23] and similarly stable using a spinning disk
335 confocal microscope [42]. Nevertheless, the photostability observed here at pH 7.4 for mEGFP is in the
336 same range as previously reported [23, 45]. Also, mGL was reported to be less photostable than Clover
337 that, in turn, is less photostable than mEGFP [21, 45], in agreement with our observations. On the other
338 hand, in contrast to our observation, Shinoda *et al.* showed that Gamillus has a 2-fold higher photostability
339 than mEGFP under widefield illumination and acidic conditions [24]. Once more, a possible explanation
340 for such discrepancies might reside in the considerably different experimental conditions which, in this
341 case, might be specifically relevant for FFS-based multimerization studies.

342 Next, we have measured the *pf* values for the different FPs, since this is a parameter of fundamental
343 importance for quantitative multimerization studies. Our results indicate that, in general, all the examined
344 FPs perform relatively well (i.e., *pf* ca. 0.7) and definitely better than most red or blue FPs [7, 19]. In
345 particular, mGL excels in this context, with a *pf* value of 0.8 and above, as confirmed by both N&B and
346 sFCS in different cell models. This might be due to its fast maturation rate [21].

347 In the second part of our work, we compared the FPs under different pH conditions. This is relevant for
348 live-cell studies with FPs targeting e.g. acidic organelles, such as endosomes, secretory granules,
349 lysosomes, and Golgi-Network (pH range ca. 4.7-8 [46]), which play a role for the sorting, transport and
350 degradation of proteins [24, 25]. In general, mNG and mGL did not exhibit a special sensitivity to changes
351 in pH values between 5.6 and 9.2. Neither of the monitored parameters (photostability, brightness or *pf*)
352 displayed a significant correlation with pH values.

353 In contrast, mEFGP showed an increase of *pf* at acidic pH, with this value being significantly higher than
354 that of Gamillus. We did not observe a strong decrease in mEGFP brightness at low pH values, as it was
355 instead previously reported [26, 28, 43, 44]. This might be due to the low laser powers employed in our
356 studies, since a control experiment performed at a ca. 4-fold higher laser power resulted in a decrease in
357 mEGFP brightness of ca. 40% (data not shown). Apart from light-induced photochemical effect, it might
358 also be possible that the data spread obtained at lower excitation power could partially mask a decrease
359 in brightness. In any case, our data show that the brightness of mEGFP at pH 5.6 is indeed slightly lower
360 than that of the other FPs.

361 Also Gamillus was influenced by changes in pH value. First, we observed that its brightness remained
362 higher than that of mEGFP, especially at low pH values. Interestingly, the photostability and the *pf*
363 decreased dramatically as a function of decreasing pH values. In contrast with the idea of Gamillus being
364 a FP particularly useful under acidic conditions [24], our data indicate that this fluorophore might perform
365 best in basic environments in the context of FFS measurements. It is possible that strong differences
366 between Gamillus and, e.g., mGFP might be observed instead at pH values below those explored in this
367 work (i.e. pH <5.5).

368 In conclusion, our results indicate that, in general, mEGFP is a very good choice for the quantification of
369 multimerization via FFS, also at pH values between 5.6 and 7.4. Although its brightness is lower than other
370 examined FPs, its remarkable photostability would allow using higher excitation powers (thus increasing
371 its brightness). At neutral pH conditions, a very good *pf* was observed for mGL, although care should be
372 taken in experiments in which photobleaching might represent an issue. Finally, at basic pH conditions
373 (e.g., up to 9.2), Gamillus represents an optimal choice based on a good photostability, high *pf* and
374 brightness.

375 Supporting Material

376 Supporting material can be found online.

377 Author Contribution

378 Research Planning, A.P., A.K.A. and S.C; Investigation, A.P. and A.K.A.; Data Analysis, A.P., A.K.A. and S.C.;
379 Writing – Original Draft Preparation, A.P.; Writing – Review & Editing, A.K.A., V.D., and S.C.; Software, V.D.,
380 A.P. and S.C.; Supervision, S.C.

381 Acknowledgements

382 We thank all the members of the Physical Biochemistry group for useful feedback. VD is grateful for
383 support by an HFSP long-term postdoctoral fellowship (HFSP LT0058/2022-L). This work was partially
384 supported by the Deutsche Forschungsgemeinschaft (DFG) project number 407961559 to S.C.

385 # References

386 1. Arant, R.J. and M.H. Ulbrich, *Deciphering the subunit composition of multimeric proteins by*
387 *counting photobleaching steps.* Chemphyschem, 2014. **15**(4): p. 600-5.
388 2. Hillesheim, L.N., Y. Chen, and J.D. Müller, *Dual-color photon counting histogram analysis of mRFP1*
389 *and EGFP in living cells.* Biophysical journal, 2006. **91**(11): p. 4273-4284.
390 3. Kuzmanov, U. and A. Emili, *Protein-protein interaction networks: probing disease mechanisms*
391 *using model systems.* Genome Medicine, 2013. **5**(4): p. 37.
392 4. Godin, A.G., et al., *Spatial Intensity Distribution Analysis Reveals Abnormal Oligomerization of*
393 *Proteins in Single Cells.* Biophys J, 2015. **109**(4): p. 710-21.
394 5. Petazzi, R.A., A.K. Aji, and S. Chiantia, *Fluorescence microscopy methods for the study of protein*
395 *oligomerization.* Prog Mol Biol Transl Sci, 2020. **169**: p. 1-41.
396 6. Bacia, K., S.A. Kim, and P. Schwille, *Fluorescence cross-correlation spectroscopy in living cells.*
397 Nature Methods, 2006. **3**(2): p. 83-89.
398 7. Dunsing, V., et al., *Optimal fluorescent protein tags for quantifying protein oligomerization in*
399 *living cells.* Sci Rep, 2018. **8**(1): p. 10634.
400 8. Chen, Y., et al., *Observing protein interactions and their stoichiometry in living cells by brightness*
401 *analysis of fluorescence fluctuation experiments.* Methods Enzymol, 2010. **472**: p. 345-63.
402 9. Chen, Y., L.N. Wei, and J.D. Müller, *Probing protein oligomerization in living cells with fluorescence*
403 *fluctuation spectroscopy.* Proc Natl Acad Sci U S A, 2003. **100**(26): p. 15492-7.
404 10. Dunsing, V. and S. Chiantia, *A Fluorescence Fluctuation Spectroscopy Assay of Protein-Protein*
405 *Interactions at Cell-Cell Contacts.* J Vis Exp, 2018(142).
406 11. Digman, M.A., et al., *Mapping the number of molecules and brightness in the laser scanning*
407 *microscope.* Biophys J, 2008. **94**(6): p. 2320-32.
408 12. Dunsing, V., A. Petrich, and S. Chiantia, *Multicolor fluorescence fluctuation spectroscopy in living*
409 *cells via spectral detection.* Elife, 2021. **10**.
410 13. Heesink, G., et al., *Quantification of Dark Protein Populations in Fluorescent Proteins by Two-Color*
411 *Coincidence Detection and Nanophotonic Manipulation.* The Journal of Physical Chemistry B,
412 2022.
413 14. Foo, Y.H., et al., *Factors affecting the quantification of biomolecular interactions by fluorescence*
414 *cross-correlation spectroscopy.* Biophys J, 2012. **102**(5): p. 1174-83.
415 15. Liebsch, F., et al., *Full-length cellular β-secretase has a trimeric subunit stoichiometry, and its*
416 *sulfur-rich transmembrane interaction site modulates cytosolic copper compartmentalization.* J
417 Biol Chem, 2017. **292**(32): p. 13258-13270.
418 16. McGuire, H., et al., *Automating single subunit counting of membrane proteins in mammalian cells.*
419 J Biol Chem, 2012. **287**(43): p. 35912-21.
420 17. Ulbrich, M.H. and E.Y. Isacoff, *Subunit counting in membrane-bound proteins.* Nat Methods, 2007.
421 **4**(4): p. 319-21.
422 18. Wu, B., Y. Chen, and J.D. Müller, *Fluorescence fluctuation spectroscopy of mCherry in living cells.*
423 Biophys J, 2009. **96**(6): p. 2391-404.
424 19. Balasubramanian, H., et al., *The dependence of EGFR oligomerization on environment and*
425 *structure: A camera-based N&B study.* Biophysical Journal, 2022. **121**: p. 4452-4466.
426 20. Schwille, P., et al., *Fluorescence correlation spectroscopy reveals fast optical excitation-driven*
427 *intramolecular dynamics of yellow fluorescent proteins.* Proc Natl Acad Sci U S A, 2000. **97**(1): p.
428 151-6.

429 21. Campbell, B.C., et al., *mGreenLantern: a bright monomeric fluorescent protein with rapid*
430 *expression and cell filling properties for neuronal imaging.* Proceedings of the National Academy
431 of Sciences, 2020. **117**(48): p. 30710.
432 22. Costantini, L.M., et al., *A palette of fluorescent proteins optimized for diverse cellular*
433 *environments.* Nat Commun, 2015. **6**: p. 7670.
434 23. Shaner, N.C., et al., *A bright monomeric green fluorescent protein derived from Branchiostoma*
435 *lanceolatum.* Nat Methods, 2013. **10**(5): p. 407-9.
436 24. Shinoda, H., et al., *Acid-Tolerant Monomeric GFP from Olindias formosa.* Cell Chemical Biology,
437 2018. **25**(3): p. 330-338.e7.
438 25. Casey, J.R., S. Grinstein, and J. Orlowski, *Sensors and regulators of intracellular pH.* Nat Rev Mol
439 Cell Biol, 2010. **11**(1): p. 50-61.
440 26. Haupts, U., et al., *Dynamics of fluorescence fluctuations in green fluorescent protein observed by*
441 *fluorescence correlation spectroscopy.* Proc Natl Acad Sci U S A, 1998. **95**(23): p. 13573-8.
442 27. Widengren, J., Ü. Mets, and R. Rigler, *Photodynamic properties of green fluorescent proteins*
443 *investigated by fluorescence correlation spectroscopy.* Chemical Physics, 1999. **250**(2): p. 171-186.
444 28. Vámosi, G., et al., *EGFP oligomers as natural fluorescence and hydrodynamic standards.* Sci Rep,
445 2016. **6**: p. 33022.
446 29. Dunsing, V., et al., *Direct evidence of amyloid precursor-like protein 1 trans interactions in cell-cell*
447 *adhesion platforms investigated via fluorescence fluctuation spectroscopy.* Mol Biol Cell, 2017.
448 **28**(25): p. 3609-3620.
449 30. Sperber, H.S., et al., *Self-association and subcellular localization of Puumala hantavirus envelope*
450 *proteins.* Sci Rep, 2019. **9**(1): p. 707.
451 31. Tzoneva, R., et al., *Effect of Erufosine on Membrane Lipid Order in Breast Cancer Cell Models.*
452 Biomolecules, 2020. **10**(5).
453 32. Petrich, A., et al., *Influenza A M2 recruits M1 to the plasma membrane: A fluorescence fluctuation*
454 *microscopy study.* Biophys J, 2021. **120**(24): p. 5478-5490.
455 33. Smith, E.M., et al., *Quantifying protein-protein interactions of peripheral membrane proteins by*
456 *fluorescence brightness analysis.* Biophys J, 2014. **107**(1): p. 66-75.
457 34. Ries, J. and P. Schwille, *Studying slow membrane dynamics with continuous wave scanning*
458 *fluorescence correlation spectroscopy.* Biophys J, 2006. **91**(5): p. 1915-24.
459 35. Balleza, E., J.M. Kim, and P. Cluzel, *Systematic characterization of maturation time of fluorescent*
460 *proteins in living cells.* Nat Methods, 2018. **15**(1): p. 47-51.
461 36. Hendrix, J., et al., *Dark states in monomeric red fluorescent proteins studied by fluorescence*
462 *correlation and single molecule spectroscopy.* Biophys J, 2008. **94**(10): p. 4103-13.
463 37. Hur, K.H., et al., *Quantitative measurement of brightness from living cells in the presence of*
464 *photodepletion.* PLoS One, 2014. **9**(5): p. e97440.
465 38. Ries, J., S. Chiantia, and P. Schwille, *Accurate determination of membrane dynamics with line-scan*
466 *FCS.* Biophysical journal, 2009. **96**(5): p. 1999-2008.
467 39. Schenk, A., et al., *Photodynamics of red fluorescent proteins studied by fluorescence correlation*
468 *spectroscopy.* Biophys J, 2004. **86**(1 Pt 1): p. 384-94.
469 40. Shaner, N.C., P.A. Steinbach, and R.Y. Tsien, *A guide to choosing fluorescent proteins.* Nat
470 Methods, 2005. **2**(12): p. 905-9.
471 41. Cranfill, P.J., et al., *Quantitative assessment of fluorescent proteins.* Nat Methods, 2016. **13**(7): p.
472 557-62.
473 42. Heppert, J.K., et al., *Comparative assessment of fluorescent proteins for in vivo imaging in an*
474 *animal model system.* Mol Biol Cell, 2016. **27**(22): p. 3385-3394.
475 43. Liu, Y., H.R. Kim, and A.A. Heikal, *Structural basis of fluorescence fluctuation dynamics of green*
476 *fluorescent proteins in acidic environments.* J Phys Chem B, 2006. **110**(47): p. 24138-46.

477 44. Steiert, F., et al., *Photophysical Behavior of mNeonGreen, an Evolutionarily Distant Green*
478 *Fluorescent Protein.* Biophys J, 2018. **114**(10): p. 2419-2431.
479 45. Lam, A.J., et al., *Improving FRET dynamic range with bright green and red fluorescent proteins.*
480 Nat Methods, 2012. **9**(10): p. 1005-12.
481 46. Theillet, F.X., et al., *Physicochemical properties of cells and their effects on intrinsically disordered*
482 *proteins (IDPs).* Chem Rev, 2014. **114**(13): p. 6661-714.

483